Dimitriadis, I., Karagianni, E., Panagiotopoulos, D., Papazachos, C., Hatzidimitriou, P., Bohnhoff, M., Rische, M., Meier, T. (2009): Seismicity and active tectonics at Coloumbo Reef (Aegean Sea, Greece): Monitoring an active volcano at Santorini Volcanic Center using a temporary seismic network. - Tectonophysics, 465, 1-4, 136-149

DOI: 10.1016/j.tecto.2008.11.005

Seismicity and active tectonics at Coloumbo Reef (Aegean Sea, Greece): Monitoring an active volcano at Santorini Volcanic Center using a temporary seismic network

I. Dimitriadis[1,*], E. Karagianni[1], D. Panagiotopoulos[1], C. Papazachos[1], P. Hatzidimitriou[1], M. Bohnhoff[2], M. Rische[3] and T. Meier[3]

[1]*Geophysical Laboratory, Department of Geology, Aristotle University of Thessaloniki, GR-54124 Thessaloniki, Greece*

[2]*GeoForschungsZentrum, Telegrafenberg D424, 14473 Potsdam, Germany*

[3]*Department of Geosciences, Ruhr-University Bochum, Germany*

Abstract

The volcanic center of Santorini Island is the most active volcano of the southern Aegean volcanic arc. A dense seismic array consisting of fourteen portable broadband seismological stations has been deployed in order to monitor and study the seismo-volcanic activity at the broader area of the Santorini volcanic center between March 2003 and September 2003. Additional recordings from a neighbouring larger scale temporary network (CYCNET) were also used for the relocation of more than 240 earthquakes recorded by both arrays. A double-difference relocation technique was used, in order to obtain optimal focal parameters for the best-constrained earthquakes.

The results indicate that the seismic activity of the Santorini volcanic center is strongly associated with the tectonic regime of the broader Southern Aegean Sea area as well as with the volcanic processes. The main cluster of the epicenters is located at the Coloumbo Reef, a submarine volcano of the volcanic system of Santorini Islands. A smaller cluster of events is located near the Anydros Islet, aligned in a NE-SW direction, running almost along the main tectonic feature of the area under study, the Santorini – Amorgos Fault Zone. In contrast, the main Santorini Island caldera is characterized by the almost complete absence of seismicity. This contrast is in very good agreement with recent volcanological and marine studies, with the Coloumbo

* Corresponding Author. Tel.: +30-2310998535 Fax: +30-2310998528

E-mail address: iordanis@geo.auth.gr (I.M. Dimitriadis)

volcanic center showing an intense high-temperature hydrothermal activity, in comparison to the corresponding low-level activity of the Santorini caldera.

The high-resolution hypocentral relocations present a clear view of the volcanic submarine structure at the Coloumbo Reef, showing that the main seismic activity is located within a very narrow vertical column, mainly at depths between 6 and 9 km. The focal mechanisms of the best-located events show that the cluster at the Coloumbo Reef is associated with the "Kameni – Coloumbo Fracture Zone", which corresponds to the western termination of the major ENE-WSW Santorini – Amorgos Fault Zone. Stress-tensor inversion of the available fault plane solutions from Coloumbo Reef, as well as existing neotectonic fault information from NE Santorini (Coloumbo peninsula), suggests that the NE Santorini – Coloumbo faults belong to a single rupture system, with a ~30^0 rotation of the local stress field with respect to the NNW-SSE regional extension field of the southern Aegean Sea. The observed change of the fault plane solutions shows that local conditions at the Coloumbo submarine volcano area control the observed faulting pattern.

Keywords: Santorini Island (Greece); Seismo-tectonic setting; Focal Mechanisms; Double-Difference earthquake relocation procedure; Stress field.

1. Introduction

One of the most prominent tectonic features of the Southern Aegean Sea is the Hellenic Arc, which consists of the forearc (Kythera, Crete, Karpathos and Rhodes) and the inner volcanic arc. African oceanic lithosphere – the northern part of the African plate – is subducting under the continental Aegean lithosphere with an approximately rate of 3.5 – 4.0 cm/a leading to the formation of an inclined Benioff seismic zone up to the depth of about 150 – 200 km (Papazachos and Comninakis, 1971; McKenzie, 1972; McClusky et al., 2000; Papazachos et al., 2000; Papazachos et al., 2005). A typical subduction related volcanic activity is also developed, with the Santorini volcanic center along with Sousaki, Methana, Milos and Nisyros forming the South Aegean Active Volcanic Arc (Georgalas, 1962; Fytikas et al., 1985). The Santorini volcanic center is recently the most active one in the Hellenic volcanic arc,

as it has erupted at least nine times during the last 600 years (1457, 1508, 1573, 1650, 1707, 1866, 1925, 1939 and 1950) (Papazachos, 1989; Fytikas et al., 1990).

The Southern Aegean is characterized by moderate to strong seismicity. Figure 1 shows important (M > 4.0) earthquakes that have been recorded during the last 50 years (Papazachos et al., 2006). In general, strong seismic activity is located along the forearc, while the back-arc region exhibits relatively low seismicity, except from the eastern part of the volcanic arc. The volcanoes, along with the clusters of epicenters of shallow and intermediate depth earthquakes form the five seismovolcanic clusters (Sousaki, Methana, Milos, Santorini and Nisyros) (Papazachos and Panagiotopoulos, 1993) (Figure 1).

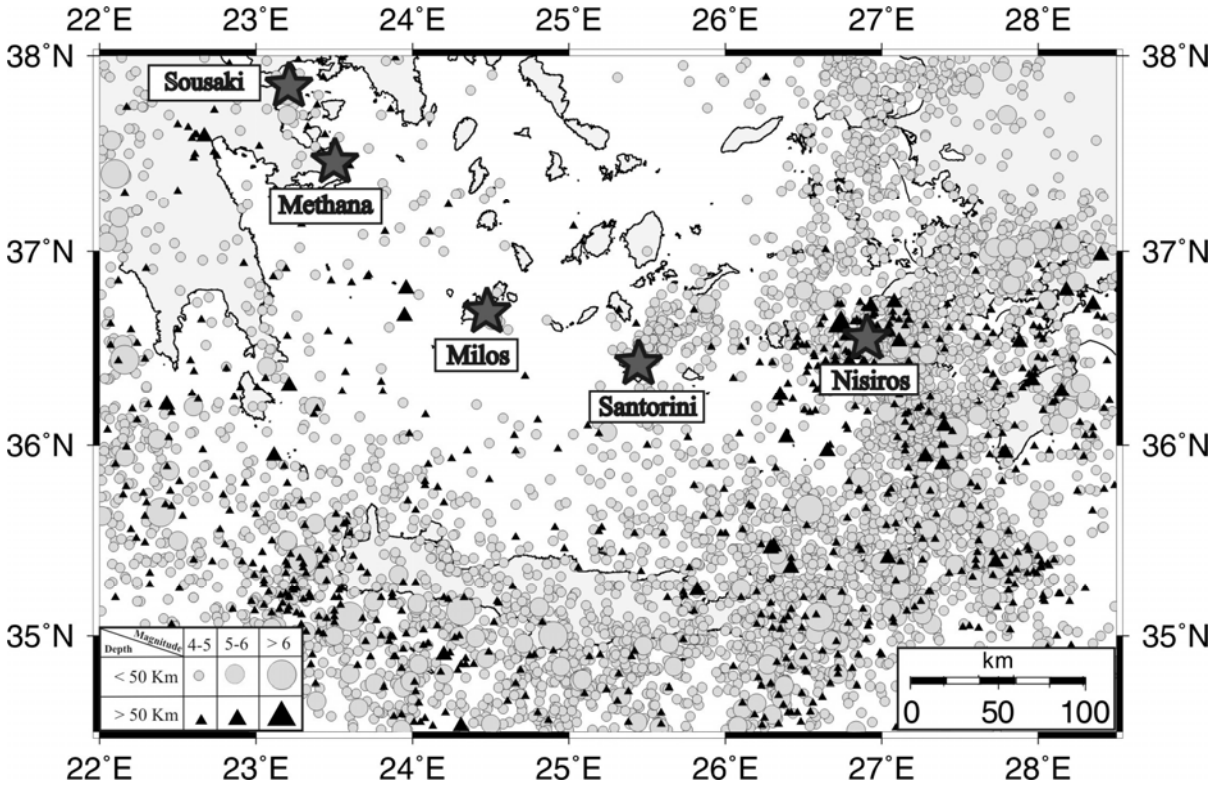

Figure 1: Seismicity map of the Southern Aegean Sea. Circles and triangles represent important (M > 4.0) shallow and intermediate depth earthquakes recorded by the regional networks during the last 50 years (Papazachos et al., 2006), respectively. Stars mark the five volcanic centers of the South Aegean Active Volcanic Arc.

The central Hellenic volcanic arc is dominated by an extensional field with a NNW – SSE direction which results in normal faults which strike ENE – WSW to NE

– SW (Kiratzi and Papazachos, 1995; Papazachos et al., 2001; Benetatos et al., 2004). In this arc, evidence for active faulting of Pliocene to Quaternary age is widespread (Perissoratis, 1990, 1995). Especially in the Santorini region changes in faulting pattern during Early Pleistocene may be related to the initiation of volcanism (Piper and Perissoratis, 2003; Piper et al., 2004). NE-trending strike-slip faulting that initiated in the latest Pliocene or early Quaternary triggered the Akrotiri volcanic center directly on Santorini Island. These faults then acted as pathways for magma, when strong NE – SW trending faulting began in the mid-Quaternary resulting in the formation of Anydros Basin, Amorgos Basin and the Santorini – Amorgos Ridge (Perissoratis, 1995; Piper and Perissoratis, 2003; Piper et al., 2004) (Figure 2).

The main tectonic feature in the broader area of Santorini volcanic center is the Santorini – Amorgos Fault Zone with an approximately ENE – WSW direction (Figure 2). This fault zone produced the two largest earthquakes which occurred in the central Aegean region during the 20th century. Both events occurred within 13 min on 9 July 1956 (the first at 03:11:40 with M = 7.5 and the second one at 03:24:03 with M = 6.9; Shirokova, 1972; Comninakis and Papazachos, 1986; Ambraseys and Jackson, 1990; Papazachos et al., 2001; Papazachos and Papazachou, 2002) generating a tsunami of up to 20 m wave heights (Papadopoulos and Pavlides, 1992; Perissoratis and Papadopoulos, 1999). Another important feature in the same area is the Coloumbo Reef (grey star in Figure 2), a submarine volcano 7 km northeast of Santorini Island which has a well defined 1500-meter-wide crater, a crater rim as shallow as 17 m and a crater floor ~500 m below the sea level (Perissoratis, 1995; Francalanci et al., 2005; Sigurdsson et al., 2006).

The Santorini volcanic center is dominated by a NNW – SSE extensional stress regime that produces various tectonic lineaments, such as the "Kameni – Coloumbo Fracture Zone" (Perissoratis, 1995; Mountrakis et al., 1996; Perissoratis and Papadopoulos, 1999; Pavlides and Valkaniotis, 2003; Piper and Perissoratis, 2003; Piper et al., 2004). This tectonic line lies in an *en echelon* pattern and is probably part of the Santorini – Amorgos Fault Zone. In particular, the area between Santorini and Amorgos Islands is dominated by an extensional field with a NNW – SSE direction which results in normal faults which strike ENE – WSW to NE – SW (Fytikas et al., 1990; Vougioukalakis et al., 1995; Mountrakis et al., 1996).

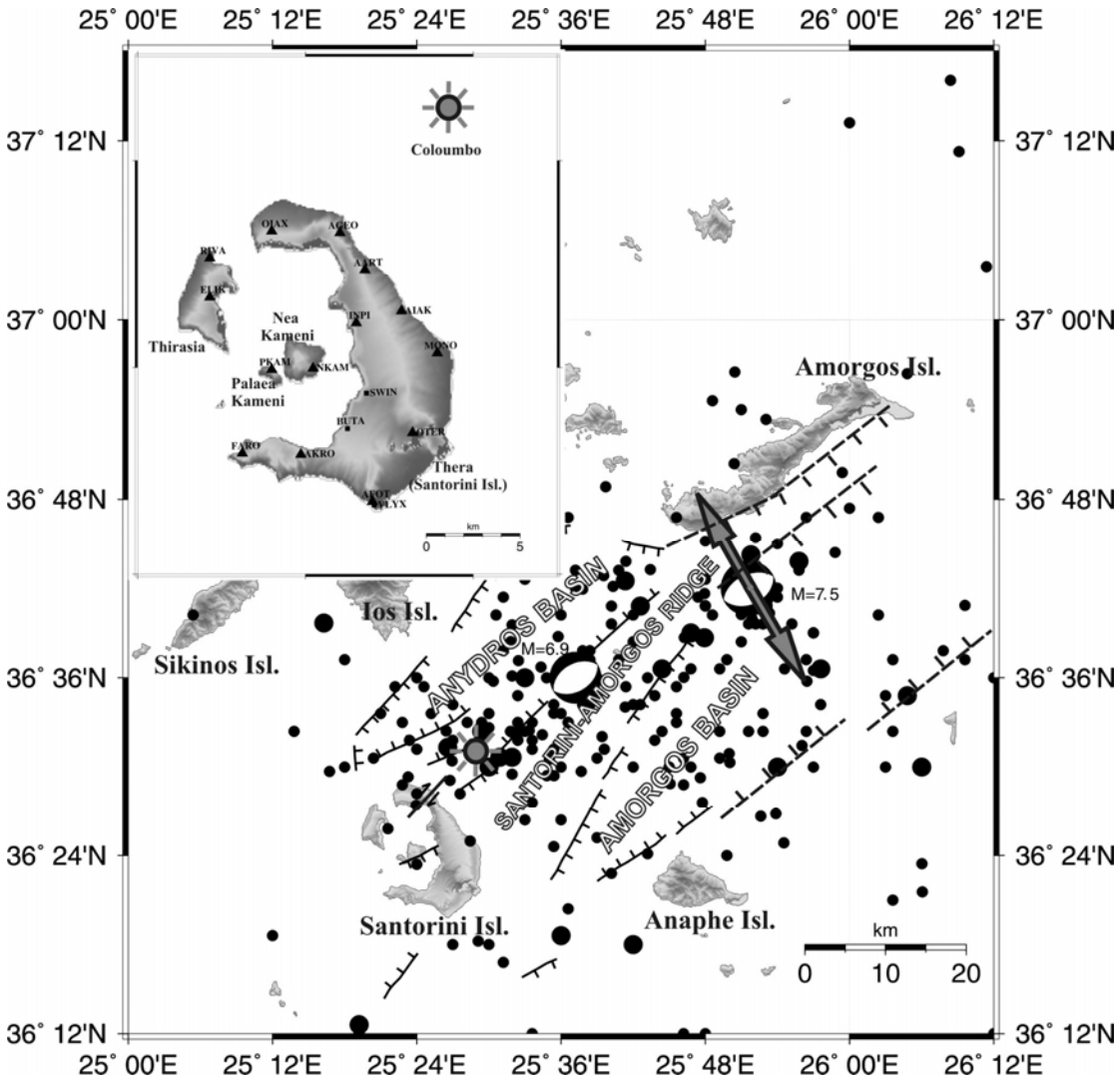

Figure 2: Map of the tectonic regime of the broader area of Santorini volcanic center, showing faults (solid lines) and probable faults (dashed lines) (modified after Perissoratis, 1995; Mountrakis et al., 1996; Perissoratis and Papadopoulos, 1999; Pavlides and Valkaniotis, 2003, Piper et al., 2004). The Coloumbo Reef is depicted by a grey star. Solid circles depict (M > 4.5) earthquakes that have been located by regional networks over the last 50 years (Papazachos et al., 2006) in the area under study. The focal mechanisms of the two large earthquakes of 1956 (M = 7.5 and M = 6.9), along with the horizontal projection of the corresponding T-axis are also depicted. In the embedded small figure the distribution of the temporary seismological stations is shown with triangles, while the squares denote the stations which have been relocated during the acquisition period (see text for details).

The broader area of Santorini volcanic center is dominated by relatively moderate to strong seismicity, which follows an ENE – WSW direction along the Santorini – Amorgos Ridge (Figures 1 and 2), as also confirmed by recent micro-seismic studies

in the area under study (e.g., Panagiotopoulos et al., 1996; Bohnhoff et al., 2004; Dimitriadis et al., 2005; Bohnhoff et al., 2006). In particular, these studies concluded that the seismic activity in the broader area of Santorini volcanic center follows a NE – SW direction along the Santorini – Amorgos Fault Zone using either the local permanent seismological network installed on the Santorini Islands (Panagiotopoulos et al., 1996; Dimitriadis et al., 2005) or a temporal seismic network installed in several islands of the Cyclades island group (CYCNET) (Bohnhoff et al., 2004, 2006). Furthermore, an important cluster of events NE of Santorini Island has been detected at the submarine volcano of Coloumbo (Dimitriadis et al., 2005; Bohnhoff et al., 2006). In this paper, we present a detailed analysis of this cluster of seismic activity using data from a local array on Santorini, as well as data from a larger scale temporary deployment (CYCNET). The seismo-tectonic interpretation is based on the seismicity distribution, as well as the source mechanisms of the larger and best-constrained events. The seismo-tectonic findings are compared with the results of previous volcanological studies of the Santorini volcanic center.

2. Seismo-volcanic Activity at Santorini Volcanic Center

2.1 Data acquisition and data processing

In order to monitor the local micro-seismic activity, a seismic array consisting of fourteen (14) broadband stations was deployed at Santorini Islands. As shown in the embedded small figure in Figure 2, the deployment of the seismic array was designed in order to cover the largest part of the Santorini volcanic center. In particular, ten stations have been installed on the Thera Island (OIAX, AGEO, AART, AIAK, INPI, MONO, SWIN, VLYX, FARO and AKRO), two stations on the Thirasia Island (RIVA and ELIK), one station on the Nea Kameni Island (NKAM) and one station on the Palaea Kameni Island (PKAM) (Figure 2). The average distance between the fourteen broadband stations was about 3 km.

This temporary seismic array was in operation from the end of March 2003 until the beginning of September 2003. During the data acquisition period, three relocations of two stations have been performed (SWIN to BUTA and to OTER and

VLYX to AFOT, see Figure 2) due to the high level of seismic "noise" in the original installation sites, as well as to achieve a better azimuthal and spatial ray coverage. Each portable seismic station was equipped with three-component broadband seismometers (CMG 40T-30s) – with the exception of two stations (MONO and INPI), which were equipped with three-component short period seismometers (CMG 40T-1s). A sampling rate of 125 Hz was used for all stations.

During the period March – September 2003, ~100 GB of continuous seismic data have been collected and the IRIS PASSCAL package software has been used to discern the seismic events from the background noise. All files have been converted to SAC format and processed by the SAC2000 (Seismic Analysis Code) computer program (Tull, 1987; Tapley and Tull, 1992) for the picking of *P*- and *S*-onset times. All events with differential $S - P$ onset times less than 10 s were considered as events of possible interest, namely candidate volcano-tectonic earthquakes and were used in the localization procedure.

2.2 Localization procedure of the volcano-tectonic earthquakes

The final data set of volcano-tectonic earthquakes recorded in the Santorini volcanic center during the period March – September 2003 consists of 243 events. The estimation of the focal parameters was performed using the computer program HYPO-ELLIPSE (Lahr, 1999) with the local velocity model of Dimitriadis et al. (2005). This model was derived using a large data set consisting of local earthquakes recorded by the local permanent seismological network (5 stations) of Santorini during the period 1994 – 2002. Due to the lack of data below 20 km, the local velocity variation from the 3-d velocity model of Papazachos and Nolet (1997) was adopted for this depth range. In order to discern the best-located events for the estimation of the focal mechanisms, as well as for the application of the double-difference technique in the relocation procedure, we selected a subset of the best-located earthquakes consisting of 159 events, which satisfy the following conditions: RMS travel time error ≤ 0.5 s, number of used phases ≥ 8, ERH (minimum horizontal error) ≤ 4 km, ERZ (minimum depth error) ≤ 6 km, minimum epicentral distance ≤ 30 km and azimuthal gap $\leq 340^0$.

The estimation of the moment magnitudes, M_w, of the best-located events has been performed using the seismological software package SEISAN version 8.0 (Havskov and Ottenmoeller, 2003). The seismic moment has been estimated using the *S*-wave displacement spectra from the horizontal components. The moment magnitude values for these events range between 0.8 and 3.6, showing relatively low-magnitude seismicity.

The epicenters of these events are shown in Figure 3. The main cluster of the seismic activity is located near the northeastern edge of the Santorini Island, at the Coloumbo Reef. Moreover, very low seismic levels are observed under the main caldera of the Santorini volcanic center during the same time period. The seismicity at Coloumbo Reef is focused, clearly associated not only with the Santorini – Amorgos Fault Zone but also with the submarine volcanic structure (Figure 3).

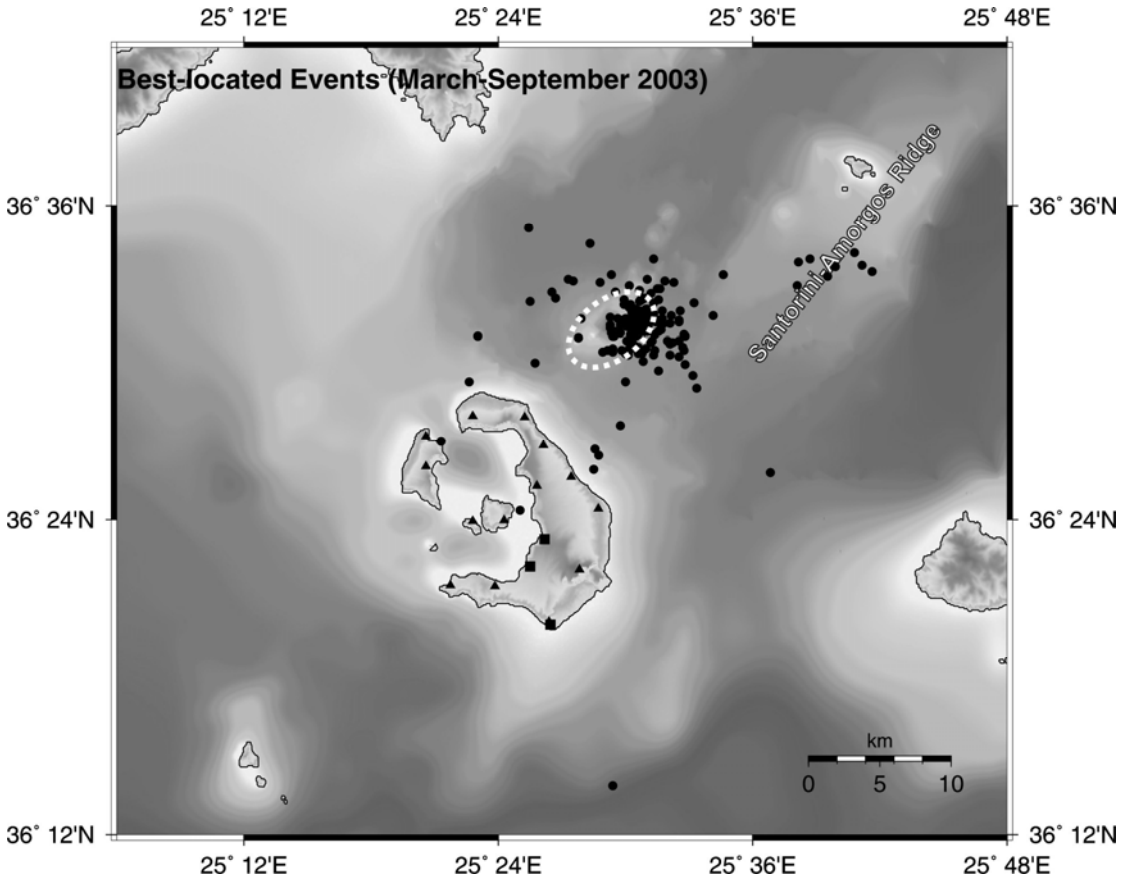

Figure 3: Epicenters of the 159 best-located events recorded during the period March – September 2003 in the area under study. Triangles represent the temporary seismological stations installed on Santorini Islands; while squares denote stations which have been relocated during the acquisition period. The Coloumbo Reef is depicted by the white ellipse (see text for details).

In order to verify and further constrain the focal parameters for the best-located events we used an independent data set from the CYCNET temporary seismological network, which temporally overlapped with our investigation. CYCNET was a 22-station network installed in the broader Cyclades area between September 2002 and July 2004 (Bohnhoff et al., 2004; Bohnhoff et al., 2006). Several stations from this array were installed in the Santorini complex and in islands surrounding it. Notice that while the local Santorini network has a poorer azimuthal coverage (stations only on Santorini) it includes a much large number of stations at small epicentral distances, whereas CYCNET has a better azimuthal coverage, with a smaller number of neighboring stations at larger epicentral distances (Figure 4).

About 130 earthquakes have been recorded by both temporary networks. For these events, we have selected seismic recordings from adjacent stations to the Santorini array, namely stations NEAK, SANC, SANN, SANS, SANT and THIR on Santorini Islands, station ANAF on Anafi Island, station IOSI on Ios Island, station ANID on Anydros Islet and stations AMOE and AMOW on Amorgos Island. All phases from the CYCNET waveform data were hand-picked again for reasons of consistency.

Using both data sets the estimation of the focal parameters was repeated using the same procedure. In Figure (4) the resulting distribution of the epicentres is shown, where the cluster at the Coloumbo Reef NE of Santorini Island is observed again as a small-scale robust feature of the seismicity. Furthermore, a small cluster of events near Anydros Islet has been relocated in a direction almost along the main tectonic feature of the area under study, the Santorini – Amorgos Fault Zone (NE – SW direction), mainly due to the data used from ANID station of CYCNET.

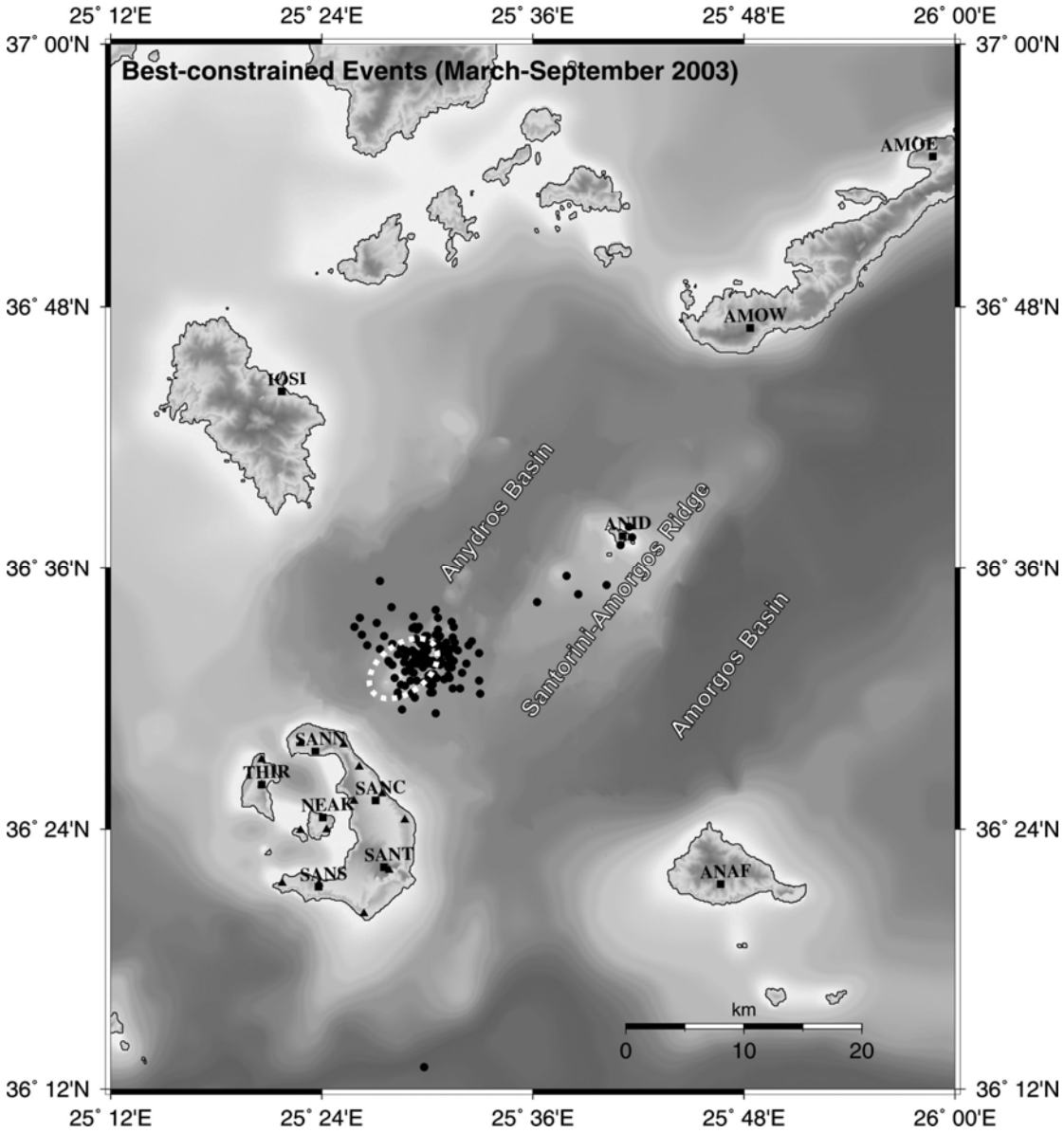

Figure 4: Epicenters of the best-constrained events using data from both seismological arrays. Black triangles represent the temporary seismological stations installed on Santorini Islands, while the black squares denote the CYCNET stations from which data have been used. The Coloumbo Reef is depicted by the white ellipse (see text for details).

2.3 Relocation of the best-constrained events

Seismicity analysis for the study of the interaction between the tectonic processes and the volcanic activity requires knowledge of the precise spatial offset between the earthquake hypocenters. The accuracy of absolute hypocenter locations is controlled

by several factors, including the network geometry, available phases, arrival-time reading accuracy, and knowledge of the crustal structure (Pavlis, 1986; Gomberg et al., 1990; Waldhauser and Ellsworth, 2000). These factors can be effectively minimized by using relative earthquake location methods (Poupinet et al., 1984; Fréchet, 1985; Frémont and Malone, 1987; Got et al., 1994). The Double-Difference (DD) earthquake relocation algorithm takes advantage of the fact that if the hypocentral separation between two earthquakes is small compared to the event-station distance and the scale length of velocity heterogeneity, then the ray paths between the source region and a common station are similar along almost the entire ray path (Waldhauser et al., 1999; Waldhauser and Ellsworth, 2000). In this case, the difference in travel times for two events observed at one station can be attributed to the spatial offset between the events with high accuracy by differencing Geiger's equation for earthquake location. The use of a 1-D model is appropriate since the DD algorithm cancels errors due to unmodeled velocity structure (Waldhauser and Ellsworth, 2002).

The relocation procedure was performed using the computer program HYPO-DD (Waldhauser, 2001) which employs the Double-Differences (DD) earthquake relocation algorithm (Waldhauser and Ellsworth, 2000). We used the final data set of the best-constrained earthquakes and obtained travel-time differences for each event pair with a separation distance less than 10 km at stations within 30 km distance from the cluster centroid (Coloumbo Reef). We employed the SVD (Singular Value Decomposition) method for HYPO-DD (Waldhauser, 2001), as it provides information on the resolution of the hypocentral parameters and the amount of information supplied by the data and adequately represents least squares errors by computing proper covariances. Furthermore, we considered that it was necessary to re-weight the residual double-difference threshold differently depending on the type of phase used. Hence, HYPO-DD was modified in order to apply different residual threshold (double residual threshold for the double-differences of the *S*-phases). Initially, we performed 5 iterations without applying any kind of cut-off parameters but only used the defaults *a priori* weights. During iterations 6 – 10 we kept the same relative *a priori* weights, but re-weighted the data for event pairs with separation distances smaller than 5 km, using a *P*-phase residual threshold of 0.25 s and an *S*-phase residual threshold equal to 0.5 s.

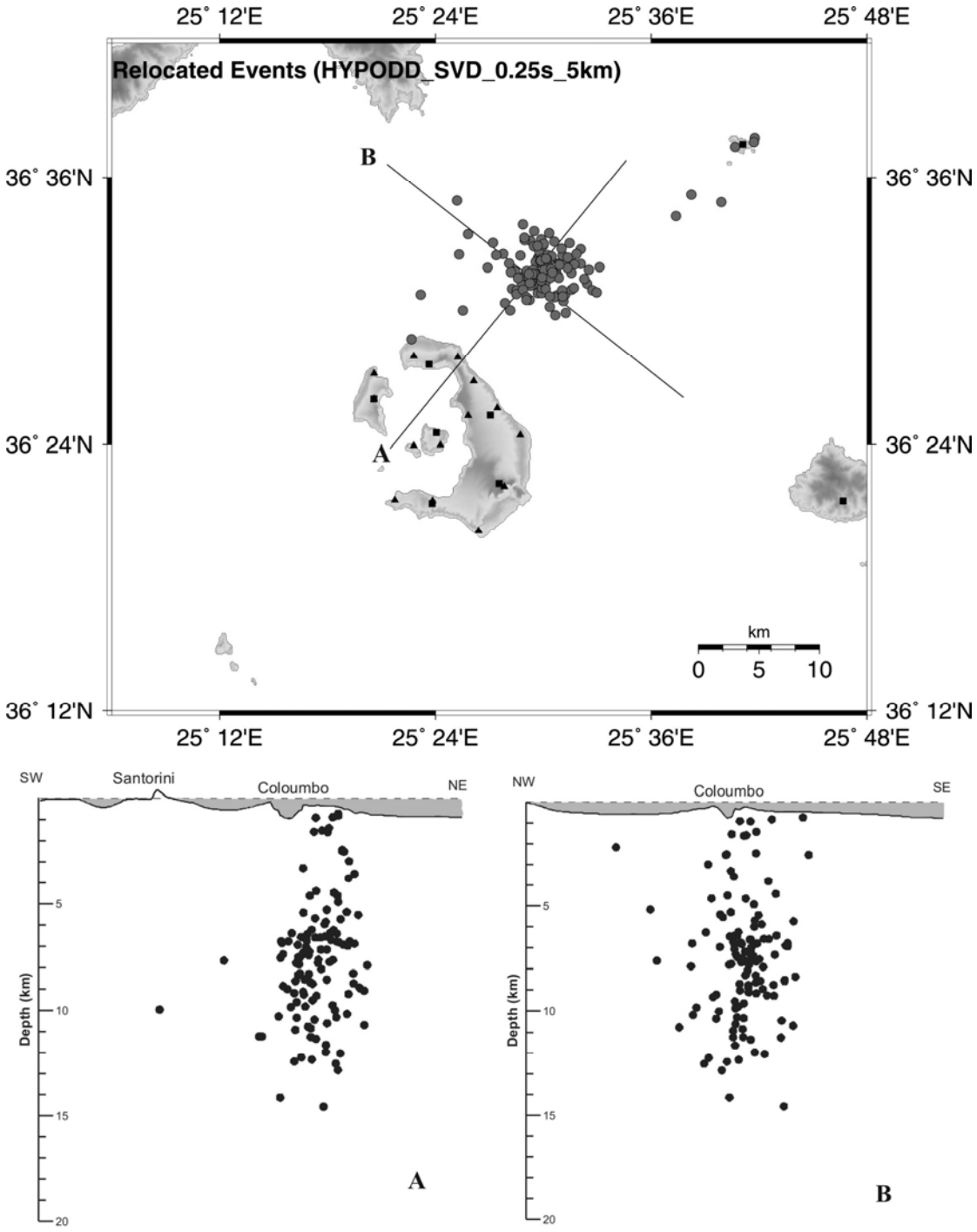

Figure 5: (Top): Epicenters of the 134 relocated events using a double-difference approach (station symbols as in Figure 4). **(Bottom):** Cross section along line A – A' (SW – NE direction) and cross section along line B – B' (NW – SE direction). The profile lengths of both lines are approximately 30 km.

The final data set of the relocated earthquakes consists of 134 events. In Figure (5) the distribution of these events is shown, while the hypocenters of the same events are presented along two cross sections. The first cross-section along line A runs parallel to the main tectonic feature of the area under study, the Santorini – Amorgos Fault Zone (NE – SW direction). The second cross section (line B) is perpendicular to the line A in a NW – SE direction (Figure 5). Both cross-sections show that the main seismic activity takes place in a narrow column with a maximum distance of 3 km from the Coloumbo Reef that extends from about 15 km depth towards the surface. The majority of events are located at depths between 6 and 9 km.

Synthetic tests were carried out to test the robustness of the obtained hypocenter locations. Using the velocity model of Dimitriadis et al. (2005) theoretical travel times were computed and uniformly distributed random errors with a standard deviation of 0.3 s for the *P*-waves travel times and of 0.3 × (*Vp/Vs*) (≈ 0.53 s) for the *S*-waves travel times was added to create the synthetic travel time data set, corresponding to an average RMS travel-time error of 0.43 s. The perturbed travel times were used in order to obtain new travel-time double differences for relocation with HYPO-DD, using the same procedure. Figure 6 shows the resulting distribution of the hypocenters along the same cross sections of the Figure 5, as well as the histograms of the time, distance and depth differences between the estimated events using the original travel times and the simulated events using the synthetic travel times. The results show that the simulated hypocenter locations are well resolved, despite a minor spatial dispersion, while the histograms show small differences in all focal parameters. In particular, the standard deviation for the origin time differences is of the order of 0.2 s, the average epicentral distance difference is of the order of 1.6 km and the standard deviation for the depth difference is of the order of 1.4 km. These tests have been repeated using the same procedure with a standard deviation of 0.5 s for the *P*-waves travel times and of 0.5 × (*Vp/Vs*) (≈ 0.89 s) for the *S*-waves travel times (average RMS travel-time error 0.72 s), leading to very similar results (standard deviation of origin time differences equal to 0.3 s, average epicentral distance difference equal to 1.9 km and standard deviation of depth difference equal to 1.9 km). Hence, the determined hypocentral distribution can be considered to be quite reliable regarding its spatial distribution.

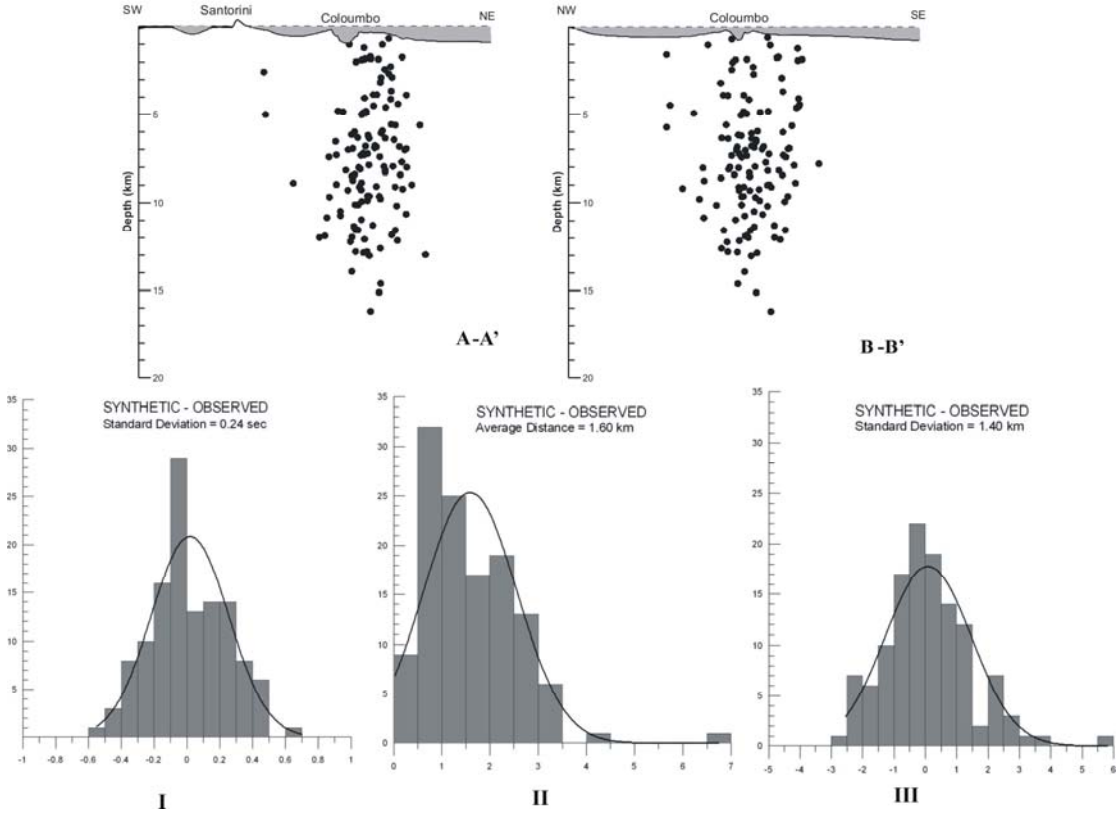

Figure 6: (Top): Cross section along line A – A' (SW – NE direction) and cross section along line B – B' (NW – SE direction) using synthetic hypocenter locations (see map in Figure 5). The profile lengths of both lines are approximately 30 km. **(Bottom):** Histograms of time (I), distance (II) and depth (III) differences between the estimated events using the original travel times and the simulated events using the synthetic travel times.

2.4 Estimation of 1-D Velocity Model

Travel times from local earthquakes provide a distributed source of elastic waves around the region under investigation, which is suitable for the joint inversion of hypocenter parameters and velocity structure (e.g., Crosson, 1976; Ellsworth, 1977; Roecker, 1982; Thurber, 1983; Kissling, 1988; Kissling et al., 1994). In the present work we have used the algorithm VELEST (Kissling et al., 1995), which allows an iterative solution to the coupled hypocenter-1-D velocity model problem and is often used for the calculation of a "Minimum" 1-D model. It performs a simultaneous

inversion for velocity model, while inversion is limited to first arriving phases (Kissling et al., 1995).

Initially, the data set of the relocated local events was used to derive *P*-velocity model using a large number of *P*-arrivals (1664 arrivals) and a fixed *Vp/Vs* ratio. Since our data set consists of earthquakes which mostly occur at depths between 6 and 9 km, this results in a relatively poor resolution for very shallow depths. Moreover, the near-vertical incidence of rays close to the surface limits the control of the shallow velocity structure. Hence, it is possible that the estimated *P*-velocities for the surface layers (~ 0 – 2 km) are biased (e.g. overestimated).

A Wadati diagram was used in order to evaluate the quality of the used phases and to obtain an appropriate *Vp/Vs* ratio. Rejection of outliers resulted in a final data set of 1566 *P*- arrivals and a *Vp/Vs* ratio of 1.76.

To probe the dependence of the solution on the initial model we have used 3 significantly different starting models: A model with various constant velocity layers and sharp velocity discontinuities, a rather smoothly varying local velocity model taken from Dimitriadis et al. (2005) and a model with an almost constant velocity gradient. For each of the three basic models we produced several additional random models by inserting random and systematic velocity perturbations at all depths, resulting in 20 new initial models for every basic initial model. The VELEST algorithm was applied for each initial velocity model and a total number of 20 final "minimum" 1-D models were derived for each case. An average *P*-velocity model was estimated in each case resulting in the three final 1-D models which are depicted in the Figure 7 with their standard deviation as horizontal errors bars. A final average *P*-velocity model was estimated for the area under study from all models (depicted by the dashed line in Figure 7d). Notice the excellent standard deviation of the order of ~0.2 km/s for the proposed velocity model (horizontal error bars).

As it is observed in Figure (7), the final 1-D model from each group of initial models, as well as the finally proposed 1-D velocity model for the area under study indicate the possible existence of at least one low-velocity layer at depths between ~ 1 and 6-7 km and a possible second low-velocity layer at depths between ~ 11 and 13 km. Although the actual velocity structure may be three dimensional, since the majority of seismicity is located in the Coloumbo Reef area, it is quite reasonable that these low-velocity layers and especially the more robust shallower one may be related

to the magmatic processes in the area of Santorini Islands and especially the Coloumbo Reef submarine volcano.

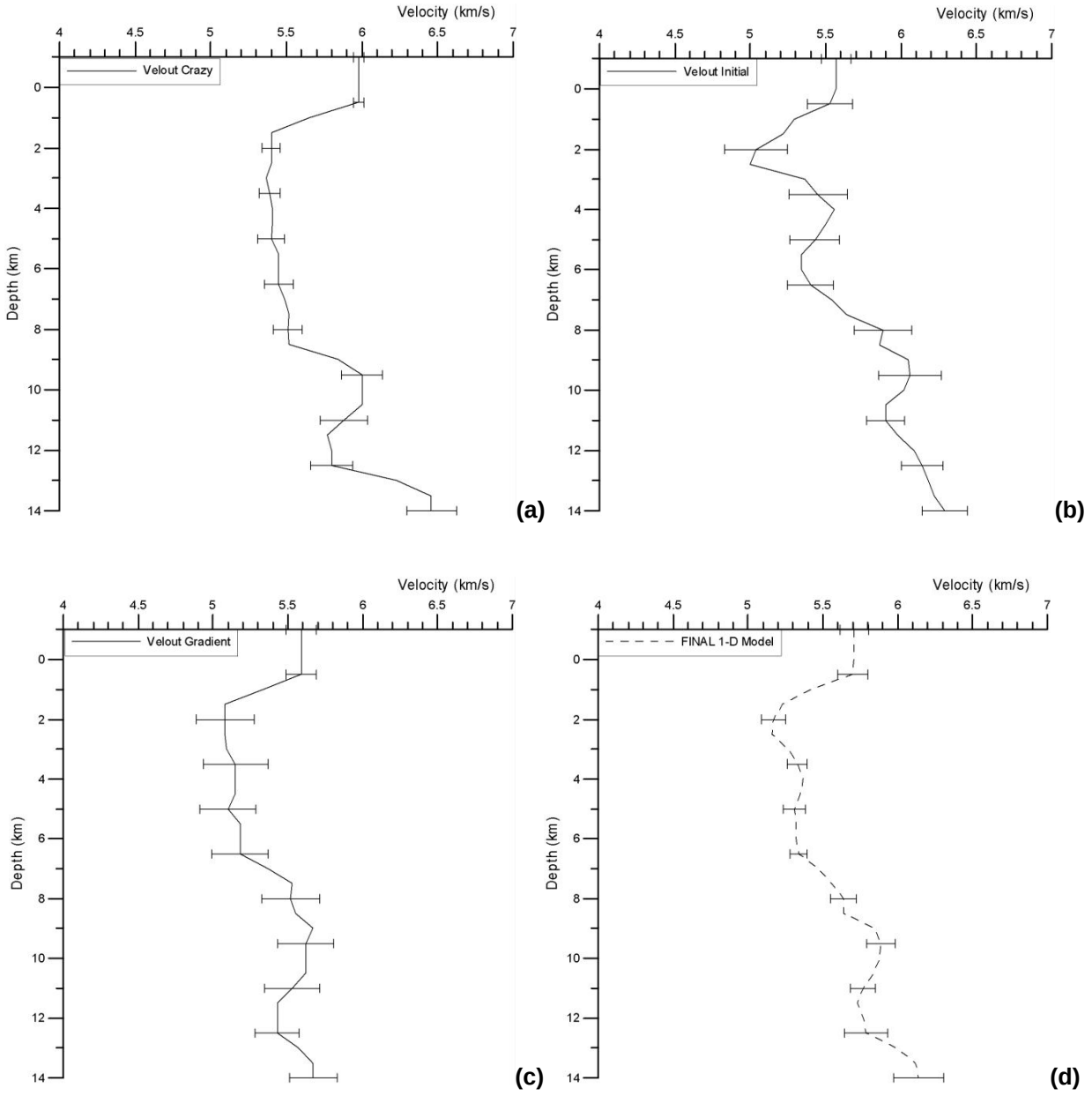

Figure 7: Estimated average final 1-D *P*-velocity model based on: **(a)** a model with sharp velocity changes with depth, **(b)** the local velocity model proposed by Dimitriadis et al. (2005) and, **(c)** an almost constant velocity gradient model. The "final" average *P*-velocity model determined for the area under study from these three initial models and their perturbations (see text for explanation) is shown in **(d)**.

3. Estimation of the focal mechanisms

Focal mechanisms were computed using the computer program FPFIT (Reasenberg and Oppenheimer, 1985), which calculates the double couple fault plane solutions based on P-wave polarity readings for the best-located earthquakes. Reliable fault plane solutions were available for 20 earthquakes, most of which have occurred at the Coloumbo Reef. These fault plane solutions show mainly dominant normal faults striking in a NE – SW direction (black beach balls in Figure 8a). Some focal mechanisms show strike–slip motions, with considerable normal component, while two mechanisms exhibit a small thrust component.

A representative "average focal mechanism tensor" was calculated using the approach of Papazachos and Kiratzi (1992) (large grey beach ball in Figure 8a). According to this method, for the determination of the stress field an average "focal mechanism" tensor is calculated. This tensor is defined by the released moment M_o and a tensor F which is a function of the strike, ζ, dip, δ, and rake, λ of the corresponding fault plane (Aki and Richards, 1980). According to the method, the eigenvalues of the average "focal mechanism" tensor $\overline{F}$ correspond to the average P, T and N (null) axes of the local stress tensor. Therefore, the method allows the definition of an "average" kinematic (P, T and N) axis which is assumed to be identical with the principal stress axes. In this approach no weighting was used since all the earthquakes used were similar, small moment magnitude events.

The focal parameters of the calculated average focal mechanism (strike = 37^0, dip = 45^0, rake = -107^0) are quite comparable with the parameters of the largest earthquake of 1956 (strike = 65^0, dip = 40^0, rake = -90^0; Shirokova, 1972; Comninakis and Papazachos, 1986; Ambraseys and Jackson, 1990; Papazachos et al., 2001). Moreover, they show an approximately 30^0 anti-clockwise rotation of the strike of normal faults at the Coloumbo Reef area. The horizontal projections of the T-axes for these mechanisms are shown in the Figure (8b), while the large grey arrow denotes the "average" kinematic T-axis (strike = 319^0, dip = 1^0).

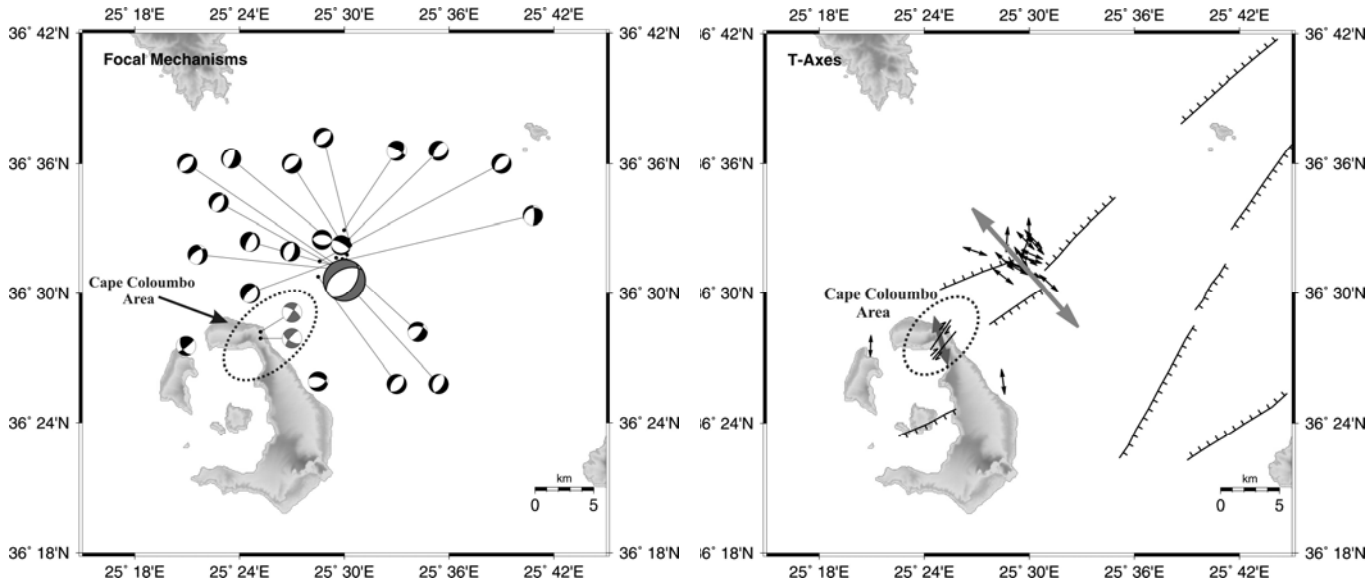

Figure 8: (a) Distributions of 20 reliable focal mechanisms for earthquakes recorded in the area under study. The average focal mechanism is shown with the large grey beach ball. The stereographic projections of the observed neotectonic faults at northeastern Thera Island (Cape Coloumbo area) are also depicted with the small grey beach balls. **(b)** Horizontal projection of T-axes for the same set of focal mechanisms, as well as the mean T-axis for the average focal mechanism (large grey arrow). Main faults of the area under study (Perissoratis, 1995; Mountrakis et al., 1996) are also depicted along with the observed stress orientation (small grey arrow) as derived by fault data.

Neotectonic and structural field observations show that the Santorini volcanic center is dominated by a NNW – SSE extensional stress regime that produces a major fault zone of NE – SW strike (approximately 35^0 – 40^0) called "Kameni – Coloumbo Fracture Zone" (Fytikas et al., 1990; Vougioukalakis et al., 1995; Mountrakis et al., 1996), which coincides with the alignment of the volcanic centers. In particular, several fault sites have been studied in the north-eastern edge of Thera Island at Cape Coloumbo area, which exhibit intense strike-slip and normal faulting in a NE – SW trending zone. A major dextral strike-slip fault zone of NE – SW strike (approximately 35^0 – 40^0) confines the deformation zone to the south, while smaller normal faults of NE – SW strike (approximately 40^0 – 70^0) belong to the same zone. In addition, the dykes present along the caldera walls in the north-eastern part of the caldera follow a main alignment of NE – SW direction, which indicates a principal

extension of NW – SE direction (Fytikas et al., 1990; Mountrakis et al., 1996). To compare these field observations with our results we present the selected faults in the Figure (8a) with the small grey beach balls, while the small grey arrow in the Figure (8b) depicts the local stress orientation as derived by the same fault data.

To quantify the compatibility of these results we applied the method of Gephart and Forsyth (1984) for inverting earthquake focal mechanism data along with fault data from field observations to obtain the local stress field. In this method the orientation of fault planes and slip directions can be used to determine best fit regional principal stress directions and the parameter $R = (\sigma_2 - \sigma_1) / (\sigma_3 - \sigma_1)$, which specifies the magnitude of the intermediate σ_2 compressive stress direction, relative to maximum σ_1 and minimum σ_3 compressive stress directions, under the assumption of uniform stress in the source region. The analysis allows for the possibility that the failure occurs on pre-existing zones of weakness of any orientation. We employed the computer program FMSI (Gephart, 1990b) to invert observations of slip directions on fault planes of known orientation in order to determine the best-fitting four-parameter stress tensor, defined by the three principal stress directions and the parameter R, as well the associated uncertainty.

For the stress inversion, as initial principal stress solution used the "average" kinematic T-axis previously estimated using the approach of Papazachos and Kiratzi (1992). The final stress model determined for the area under study corresponds to value of R equal to 0.4 and the determined orientation of the mean extensional stress axis (strike = 311^0, dip = 18^0) is almost identical to the estimated "average" kinematic T-axis (strike = 319^0, dip = 1^0) using the approach of Papazachos and Kiratzi (1992).

The application of the stress-tensor inversion allowed choosing the plane corresponding to the minimum misfit rotation about an axis of general orientation which is needed to match an observed fault plane / slip direction with one consistent with the final stress model. These faults are identified by the inversion method to be the "ideal" fault planes on which the corresponding earthquakes occurred. However, it is clear that this selection is arbitrary if both nodal planes exhibit similar misfit values which are either small (both planes are acceptable) or very large (both could be considered as "incompatible" with the determined stress field). Taking into account the average uncertainty of 10° related with the provided fault plane solutions and their kinematic axes, we can consider the difference of the misfit values of the two planes provided by the method as a quality measure for the selection procedure. In order to

obtain more realistic and reliable results we have assumed that if the misfit calculated for both fault planes (main and auxiliary) is relatively small (less than 2–3 times larger than the average uncertainty, i.e. 25°) and their difference is less than the average uncertainty (10°), then both planes should be considered and included in the results of this study, as they are practically indistinguishable with respect to their misfit using the determined stress field. Nine (9) fault plane solutions showed a rotation misfit less than 10° for both nodal planes, hence use both planes were adopted as candidate faults. For larger rotation misfit difference values (larger than 10°), we took the traditional approach and kept the plane which was most compatible with the determined stress field (smaller misfit). Eleven (11) focal mechanisms showed a rotation misfit larger than 10° but significantly smaller than 25° for at least one of the two fault planes, which was the one adopted as the fault plane optimally oriented to the determined stress field.

In Figure 9 fault planes identified by the stress inversion are presented as linear elements, along with the determined orientation of the mean extensional axis presented as the large grey arrow. The distribution of the identified faults is also presented with a rosediagram, which is showing the dominant NE – SW (30^0 – 45^0) trending faults. In most cases, the faults "proposed" by the inversion method are in agreement with the faults observed in the field or with the expected directions of the faults, as these are depicted by the seismicity distribution. It is very interesting to notice that both the neotectonic field observations (in the ellipse in Figure 9) and the fault planes from earthquake data are compatible with a single extensional stress field with a NW – SE direction, despite the different type of fault-slipping observed in the two data sets. This compatibility suggests that the Santorini – Coloumbo faults belong to a single rupture system, where local conditions at the Coloumbo submarine volcano area control and modify the faulting pattern from trans-tensional to almost purely normal (Figure 9).

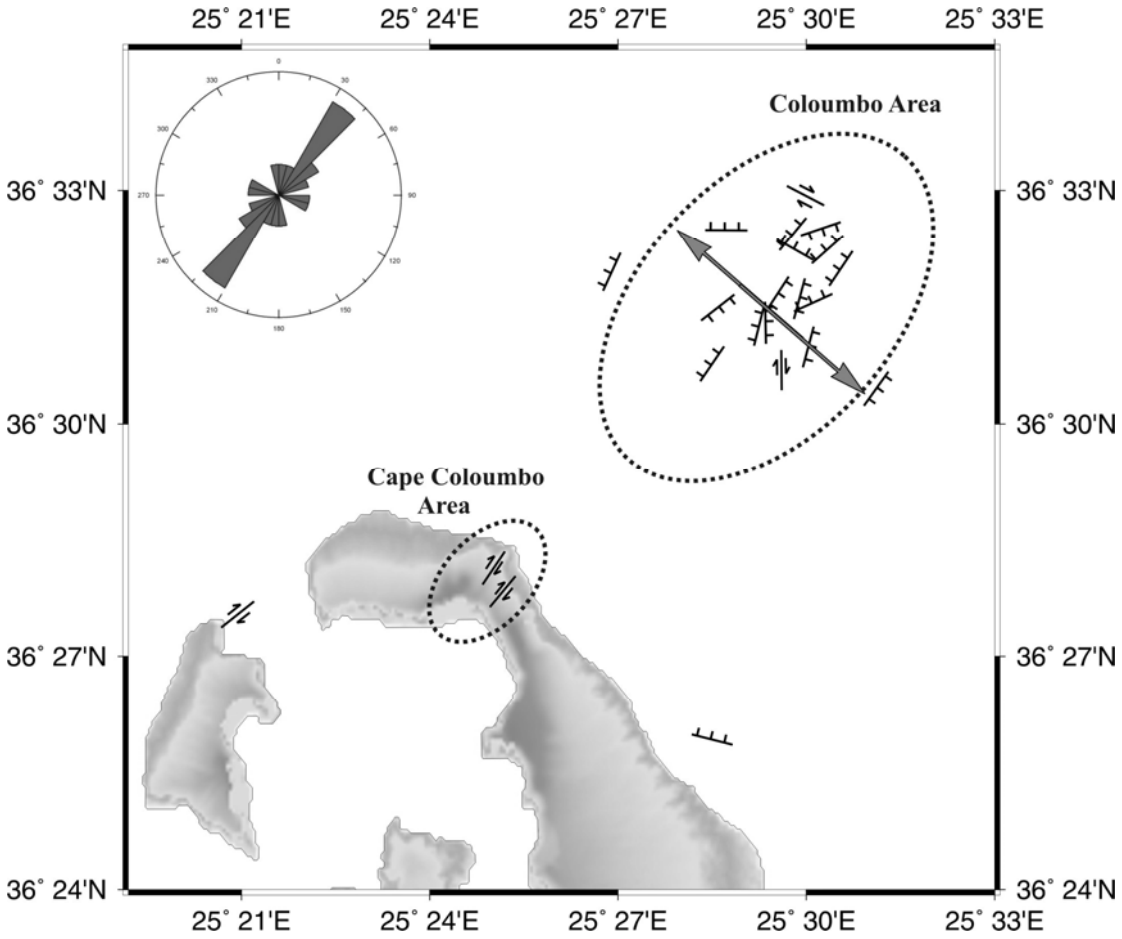

Figure 9: Fault planes identified by the stress tensor inversion method as candidates for the "real" seismic faults, using both seismological and neotectonic data. The rosediagram presents the azimuthal fault distribution, while the large grey arrow depicts the determined orientation of the mean extensional stress axis.

4. Discussion and Conclusions

The results obtained in the present study show that the main seismic activity of the Santorini volcanic center during the period March – September 2003 is associated mainly with the tectonic regime of the broader area under study, as well as with the recently observed high hydrothermal activity at Coloumbo Reef area (Sigurdsson et al., 2006). In particular, the main cluster of the epicenters is located near the north-eastern edge of the Santorini Island beneath the Coloumbo Reef, where a 3 km wide column of micro-seismicity extends from about 15 km depth towards the surface. The highest concentration of hypocenters is observed mainly at depths between 6 and 9

km. The hypocenters of this cluster are located mostly beneath the north-eastern part of the Coloumbo volcano's crater (Figure 5). In contrast, there is no evidence of seismic activity beneath the caldera of the Santorini volcano. This observation is in very good agreement with recent results for the same area (e.g., Dimitriadis et al., 2005; Bohnhoff et al., 2004, 2006; Hensch et al., 2008).

Recent marine investigations in the area under study discovered a widespread hydrothermal vent field on the floor of the Coloumbo volcano's crater, especially, in the northern part of this crater, with vigorous gas emission plumes more than 10 meters above the floor and fluid temperatures up to 220ºC from vent chimneys up to four meters high (Sigurdsson et al., 2006). In contrast to the high-temperature venting in Coloumbo Reef area, only low-temperature venting was observed within the Santorini caldera by the same marine survey (fluid temperatures around 15º – 17ºC) (Sigurdsson et al., 2006) (Figure 10). The difference of hydrothermal activity in the Santorini caldera versus the Coloumbo crater is in agreement with the lack of seismicity observed beneath the Santorini caldera in comparison with the strong seismicity observed in the area of Coloumbo Reef. The high-temperature hydrothermal field in the northern part of the Coloumbo's crater could be linked with the "column" of events beneath this point (Figure 5).

The main body of the seismic activity under the Coloumbo Reef is observed mostly at depths 6 – 9 km, almost in anti-correlation with the indications of the presence of low-velocity layers, which may indicate the presence of shallow magmatic chambers (Figures 5 and 7). Since the mean thickness of the crust beneath Santorini is about 25 km (Papazachos and Nolet, 1997; Bohnhoff et al., 2001; Karagianni et al., 2002; Papazachos et al., 2005) and the observed micro-seismicity in this area does not extend deeper than 15 km, it can be concluded that the thermo-mechanical properties of the lower crust in the area do not allow the generation of significant earthquake activity. This assumption is also supported by the magmatic evolution occurring in reservoirs sited at different levels in the crust that has been suggested for the Santorini volcanic center (e.g., Huijsmans et al., 1988; Vougioukalakis et al., 1995; Druitt et al., 1999; Mortazavi and Sparks, 2004; Francalanci et al., 2005; Zellmer et al., 2005). It should be noted that recent volcanological and geochemical studies suggest the presence of different magmatic reservoirs beneath Santorini caldera and Coloumbo submarine volcano, respectively (Vougioukalakis et al., 1995; Francalanci et al., 2005). In particular, according to

these studies, the magmatic chambers appear to have different geochemical and mineralogical characteristics, indicating possibly a different magmatism, derived directly from the mantle for the case of Coloumbo submarine volcano and with significant partial crustal melting for the case of the Santorini caldera (Figure 10) (Vougioukalakis et al., 1995; Francalanci et al., 2005).

The focal mechanisms of the best-located events show a dominant normal faulting pattern with a NW-SE extension and NE-SW fault planes. This observation suggests that the cluster at Coloumbo Reef is connected with the "Kameni – Coloumbo Fracture Zone" (NE – SW direction). A representative "average focal mechanism tensor" derived from the reliable fault plane solutions in the Coloumbo area is in good agreement with both focal mechanisms from the two main earthquakes occurred in 1956 (Shirokova, 1972; Comninakis and Papazachos, 1986; Ambraseys and Jackson, 1990; Papazachos et al., 2001; Papazachos and Papazachou, 2002). Furthermore, the application of the stress inversion method of Gephart and Forsyth (1984) shows that both the seismological data and the available neotectonic observations at the north-eastern part of Santorini Island can be explained by a single stress field, despite the local faulting variations of the Santorini – Coloumbo rupture zone and around Coloumbo Reef.

A rotation of the determined orientation of the mean extensional axis of the order of ~ 30^0 in comparison to the 1956 events is observed in the vicinity of the Santorini – Coloumbo area. In particular, a change of the main strike of the Santorini – Amorgos Fault Zone is observed at the western termination of the zone at the Coloumbo – Santorini area. This "bending" to NE-SW faulting at Coloumbo – Santorini area is in agreement with the recent suggestion of Papazachos et al. (2001) for the broader study area and is frequently observed in the broader Aegean area at the termination of E-W or ENE-WSW faults (e.g., Kozani area – Northern part of Greece, Kiratzi, 1999). Moreover, this change is often accompanied by a change of the faulting pattern from normal to oblique (dextral-normal) slip. In the Kameni – Coloumbo area this does not occur at the Coloumbo Reef, probably due to the combination of active faulting and local volcanic processes, which result in an "opening" of the fault zone with a dominant normal faulting (Figure 10). However, towards Santorini field observations (Mountrakis et al., 1996) strongly suggest that faulting does change to a more oblique type, with a strong dominant dextral slip component (Figure 10).

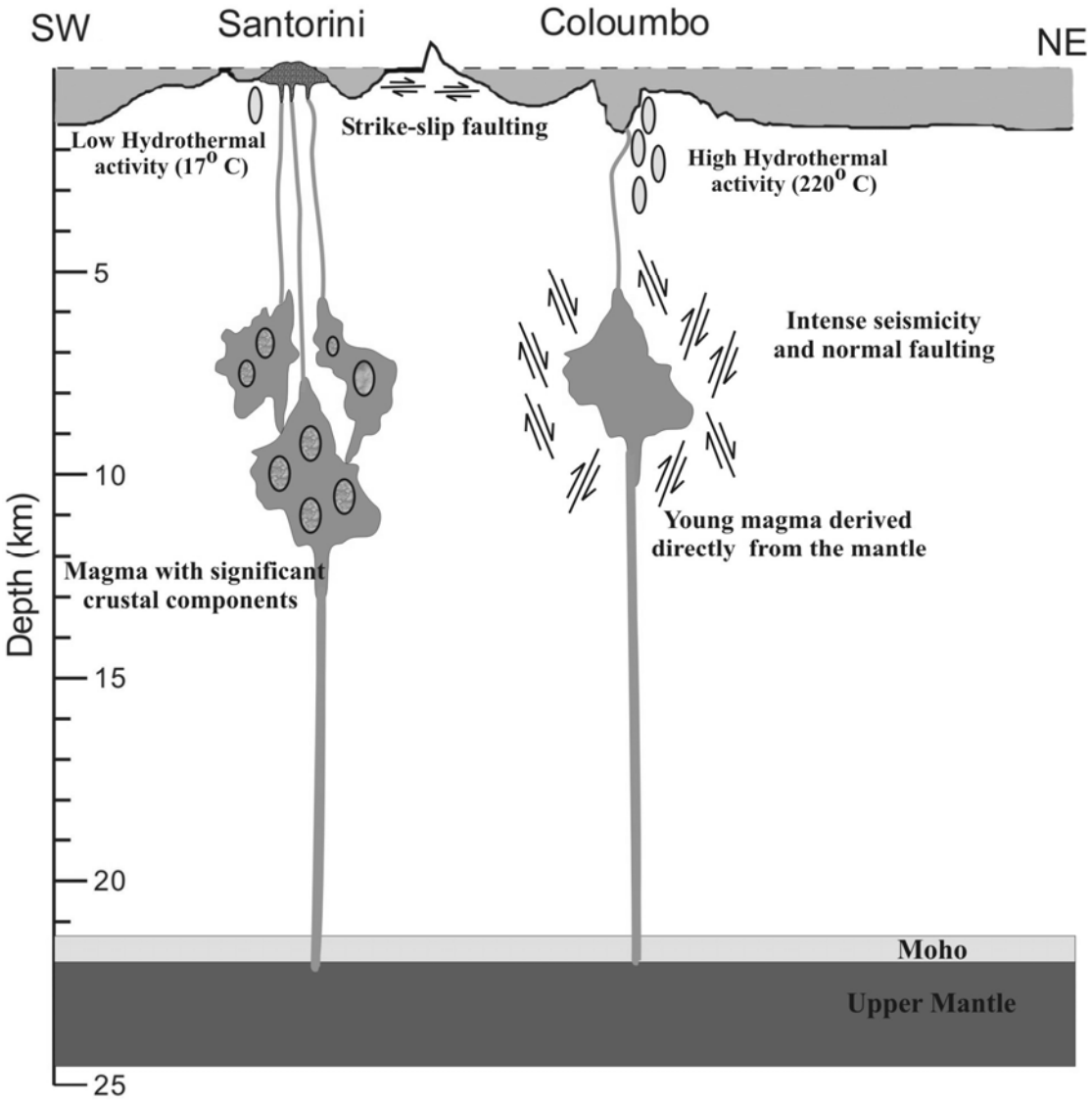

Figure 10: Depth section along a 45 km SW – NE trending profile from the Santorini Island towards the Coloumbo area showing a schematic model of the volcano-tectonic processes taking place in the study area. On the basis of results obtained in this work, as well as recent volcanological and geochemical studies, different volcano-tectonic processes are taking place beneath Santorini caldera and Coloumbo submarine volcano, respectively (see text for details).

Since the average focal mechanism probably reflects the typical regional stress field, it can be assumed that the resulting Santorini-Amorgos fault zone provides pathways for ascending dykes. The column-like cluster of micro-seismicity beneath Coloumbo Reef is very likely triggered by magmatic processes, whereas the large earthquakes in 1956 are a response to tectonic loading. The magmatic processes

beneath Coloumbo Reef locally modify the faulting pattern and stress field, as evident from the variable source mechanisms. Further long-term observations are necessary in order to monitor the space-time evolution of the seismo-volcanic activity beneath Coloumbo submarine volcano.

ACKNOWLEDGEMENTS

This work was partially funded by the e-Ruption E.C. Project (EVR1-2001-00024) and the PYTHAGORAS research program of the Hellenic Ministry of Education (Research Committee of University of Thessaloniki #21945#). We are grateful to Thanasis Karamesinis, Stylianos Koutrakis, Kiriakos Peftitselis and Domenikos Vamvakaris for their help in the field. We would also like to thank the Institute for the Study and Monitoring of the Santorini Volcano (ISMOSAV), Santorini, Greece, as well as M. Fytikas and I. Kotiadis for helping us to install and to maintain the temporary seismic array on the Santorini Islands. Furthermore, we would like to thank Professors J.M. Ibanez and G. Alguacil of the University of Granada, Spain, for their contribution to the moment magnitude estimation.

REFERENCES

Aki, K. and Richards, P., 1980. Quantative Seismology: Theory and Methods. *Freeman, San Francisco, California*, pp. 557.

Ambraseys, N. N. and Jackson, J., 1990. Seismicity and associated strain of central Greece between 1890 and 1988. *Geophys. J. Int., 101*, pp. 663-708.

Benetatos, C., Kiratzi, A., Papazachos C., and Karakaisis, G., 2004. Focal mechanisms of shallow and intermediate depth earthquakes along the Hellenic Arc. *J. of Geodyn. 37*, pp. 253–296.

Bohnhoff, M., Makris, J., Stavrakakis, G., and Papanikolaou, D., 2001. Crustal investigation of the Hellenic subduction zone using wide aperture seismic data. *Tectonophysics 343*, pp. 239–262.

Bohnhoff, M., Rische, M., Meier, T., Endrun, B., Harjes, H.-P., Stavrakakis, G., 2004. A temporary seismic network on the Cyclades (Aegean Sea, Greece). *Seismol. Res. Letters 75/3*, pp. 352–357.

Bohnhoff, M., Rische, M., Meier, T., Becker, D., Stavrakakis G., and Harjes, H.-P., 2006. Microseismic activity in the Hellenic Volcanic Arc, Greece, with emphasis on the seismotectonic setting of the Santorini-Amorgos zone. *Tectonophysics 423, Issues 1-4*, pp. 17-33.

Comninakis, P. E. and Papazachos, B. C., 1986. A catalogue of earthquakes in Greece and the surrounding area for the period 1901-1985. *Univ. Thessaloniki Geophys. Lab. Publ*, Thessaloniki, Greece.

Crosson, R.S., 1976. Crustal Structure Modeling of Earthquake Data, 1, Simultaneous Least Squares Estimation of Hypocenter and Velocity Parameters. *Journal of Geophysical Research 81*, pp. 3036-3046.

Dimitriadis I.M., Panagiotopoulos D.G., Papazachos C.B., Hatzidimitriou P.M., Karagianni E.E. and Kane I., 2005. Recent seismic activity (1994-2002) of the Santorini volcano using data from local seismological network. *The South Aegean Active Volcanic Arc: Present Knowledge and Future Perspectives (Developments in Volcanology, Volume 7),* pp. 185-203.

Druitt T.H., Davies, M.S., Edwards, L., Sparks, R.S.J., Mellors, R.M., Pyle, D.M., Lanphere, M. and Barreirio, B., 1999. The Santorini Volcano. *Geological Society Special Memoir, 19*, *Geological Society Pub House, London*.

Ellsworth, W.L., 1977. Three-dimensional structure of the crust and mantle beneath the island of Hawaii. *Ph.D. Thesis, Massachusetts Institute of Technology, Cambridge*, p. 327.

Francalanci, L., Vougioukalakis, G., Perini, G. and Manetti, P., 2005. A West-East Traverse along the magmatism of the south Aegean volcanic arc in the light of volcanological, chemical and isotope data. *The South Aegean Active Volcanic Arc: Present Knowledge and Future Perspectives (Developments in Volcanology, Volume 7),* pp. 65-111.

Fréchet, J., 1985. Sismogenèse et doublets sismiques, thèse d'Etat, *Univ. Sci. et Méd. de Grenoble, Grenoble, France*, pp. 206.

Frémont, M. -J., and Malone S. D., 1987. High precision Relative locations of earthquakes at Mount St. Helens, Washington. *J. Geophys. Res. 92*, pp. 10,223–10,236.

Fytikas, M., Innocenti, F., Manetti, P., Mazzuoli, R., Peccerillo, A. and Villari, L., 1985. Tertiary to Quaternary evolution of volcanism in the Aegean region. *In: The Geological Evolution of the Eastern Mediterranean, Special Publ. Geol. Soc., 17:* pp. 687-699.

Fytikas, M., Kolios, N. and Vougioukalakis, G., 1990. Post-Minoan Volcanic Activity of the Santorini Volcano. Volcanic hazard and risk, forecasting possibilities. *In: Hardy, D.A., (Editor), Thera and the Aegean World III, 2. The Thera Foundation, London*, pp. 183-198.

Georgalas, G.C., 1962. Active volcanoes in the world including solfatara fields. *Intern. Volcan. Assoc., 12*: pp. 1-40.

Gephart, J. W., 1990b. FMSI: a FORTRAN program for inverting fault slickenside and earthquake focal mechanism data to obtain the regional stress tensor. *Comput. Geosci., 16 (7)*, pp. 953-989.

Gephart, J. W., and Forsyth, D. W., 1984. An improved method for determining the regional stress tensor using earthquake focal mechanism data: application to the San Fernando earthquake sequence. *J. Geophys. Res. 89 (B11)*, pp. 9305-9320.

Gomberg, J. S., K. M. Shedlock, and S. W. Roecker, 1990. The effect of S-wave arrival times on the accuracy of hypocenter estimation. Bull. *Seism. Soc. Am. 80*, pp. 1605-1628.

Got, J. -L., Fréchet, J. and Klein, F. W., 1994. Deep fault plane geometry inferred from multiplet relative relocation beneath the south flank of Kilauea. *J. Geophys. Res., 99*, pp. 15,375– 15,386.

Havskov, J. and L. Ottemoeller, 2003. The SEISAN: Earthquake analysis software for Windows, Solaris, Linux and Macosx (Version 8.0), Manual and software, Institute of Solid Earth Physics, University of Bergen.

Hensch, M., Dahm, T., Hort, M., Dehghani, A., Hübscher, C., and the EGELADOS working group, 2008. First results of the Ocean-Bottom-Seismometer and-Tiltmeter experiment at Columbo submarine volcano (Aegean Sea, Greece), Geophysical Research Abstracts, Vol. 10, EGU2008-A-02760, EGU General Assembly 2008.

Huijsmans, J., Barton, M. and Salters, V., 1988. Geochemistry and evolution of the calc-alkaline volcanic complex of Santorini, Aegean Sea, Greece. *J. Volcanol. Geotherm. Res., 34*, pp. 283-306.

Karagianni, E. E., Panagiotopoulos, D. G., Panza, G. F., Suhadolc, P., Papazachos, C. B., Papazachos, B. C., Kiratzi, A., Hatzfeld, D., Makropoulos, K., Priestley, K. and Vuan, A., 2002. Rayleigh wave group velocity tomography in the Aegean area. *Tectonophysics 358*, pp. 187-209.

Kiratzi, A. A., 1999. Stress tensor inversion in Western Greece using earthquake focal mechanisms from the Kozani–Grevena 1995 seismic sequence. *Ann. Geophys. 42, (4)*.

Kiratzi, A. A., and Papazachos, C. B. 1995. Active seismic deformation in the southern Aegean Benioff zone. *J. Geodynamics, 19*, pp. 65-78.

Kissling, E., 1988. Geotomography with local earthquake data. *Rev. Geophys., 26*, pp. 659-698.

Kissling, E., Ellsworth, W.L., Eberhart-Phillips, D. and Kradolfer, U., 1994. Initial reference models in local earthquake tomography. *Journal of Geophysical Research 99*, pp. 19'635-19'646.

Kissling, E., Kradolfer, U., and Maurer, H., 1995. VELEST User's Guide (Version 3.1). *Institute of Geophysics, ETH Zurich*.

Lahr, J.C., 1999. HYPO-ELLIPSE/Version 1.0: A computer program for determining local earthquake hypocentral parameters, magnitude, and first-motion pattern (Y2K Compliant Version). *U.S. Geological Survey Open-File Report 99-23.*

McClusky, S. Balasdsanian, A. Barka, C. Demir, I. Georgiev, M. Hamburger, K. Hurst, K. Kastens, G. Kekelidze, R.K.V. Kotzev, O. Lenk, S. Mahmoud, A. Mishin, M. Nadariya, A. Ouzounis, D. Paradissis, Y. Peter, M. Prilepin, R. Reilinger, I. Sanli, H. Seeger, A. Tealeb, M.N. Toksoz and G. Veis, 2000. Global positioning system constraints on crustal movements and deformations in the eastern Mediterranean and Caucasus. *Journal of Geophysical Research 105,* pp. 5695–5719.

McKenzie, D.P., 1972. Active tectonics of the Mediterranean region. *Geophys. J.R. Astr. Soc., 30*: pp. 109-185.

Mortazavi, M. and Sparks, R.S.J., 2004. Origin of rhyolite and rhyodacite lavas and associated mafic inclusions of Cape Akrotiri, Santorini: the role of wet basalt in

generating calc-alkaline silicic magmas. *Contrib. Mineral. Petrol., 146*, pp. 397-413.

Mountrakis, D. M., Pavlides, S. B., Chatzipetros, A., Meletlidis, S., Tranos, M. D., Vougioukalakis, G. and Kilias, A. A., 1996. Active deformation of Santorini. *Proceedings of 2nd Workshop on European Laboratory Volcanoes, May 2-4 1996, Santorini, Greece*, pp. 13-22.

Panagiotopoulos, D.G., Stavrakakis, G., Makropoulos, K., Papanastasiou, D., Papazachos, C.B., Savvaidis, A.S. and Karagianni, E.E., 1996. Seismic monitoring at the Santorini volcano. *Proceedings of 2nd Workshop on European Laboratory Volcanoes, May 2-4 1996, Santorini, Greece*, pp. 311-324.

Papadopoulos, G. A., and Pavlides, S. B., 1992. The large 1956 earthquake in the South Aegean: Macroseismic field configuration, faulting, and neotectonics of Amorgos Island, *Earth and Planetary Science Letters*, *Volume 113, Issue 3*, pp. 383-396.

Papazachos, B.C. and Comninakis, P.E., 1971. Geophysical and tectonic features of the Aegean arc. *Journal of Geophysical Research 76*, pp. 8517-8533.

Papazachos, B.C., 1989. Long and short term prediction of the volcanic eruptions in Santorini. *In: Proceedings of 3rd International Congress "Thera and the Aegean World III", Volume 2, September 4-8 1989, Santorini, Greece*, pp. 125-129.

Papazachos, B.C. and Panagiotopoulos, D.G., 1993. Normal faults associated with volcanic activity and deep rupture zones in the southern Aegean volcanic arc. *Tectonophysics 220*, pp. 301-308.

Papazachos, B.C., Karakostas, V.G., Papazachos, C.B. and Scordilis, E.M., 2000. The geometry of the Wadati-Benioff zone and lithospheric kinematics in the Hellenic arc. *Tectonophysics, 319,* pp. 275-300.

Papazachos, B.C., Mountrakis, D.M., Papazachos C.B., Tranos, M.D., Karakaisis, G.F. and Savvaidis, A.S., 2001. The fault which have caused the known major earthquakes in Greece and surrounding region between the 5th century BC and today. *Proceedings of 2nd National Conference Anti-Seismic Engineering and Technical Seismology, November 28-30, 2001, Thessaloniki, Greece,* pp. 17-26.

Papazachos, B.C. and Papazachou, C.B., 2002. The Earthquakes of Greece. *Ziti Publications*, Thessaloniki, Greece.

Papazachos, B.C., Dimitriadis, S.T., Panagiotopoulos, D.G., Papazachos, C.B. and Papadimitriou, E.E., 2005. Deep structure and active tectonics of the southern Aegean volcanic arc. *The South Aegean Active Volcanic Arc: Present Knowledge and Future Perspectives (Developments in Volcanology, Volume 7),* pp. 47-64.

Papazachos, B.C., Comninakis, P.E., Scordilis, E.M., Karakaisis, G.F. and C.B. Papazachos, 2006. A catalogue of earthquakes in the Mediterranean and surrounding area for the period 1901 – 2005. *Publ. Geophysical Laboratory, University of Thessaloniki*.

Papazachos, C. B. and Kiratzi, A., 1992. A formulation for reliable estimation of active crustal deformation and its application to central Greece. *Geophys. J. Int. 111*, pp. 424-432.

Papazachos, C. B. and Nolet, G., 1997. *P* and *S* deep structure of the Hellenic area obtained by robust nonlinear inversion of travel times. *Journal of Geophysical Research 102*, pp. 8349-8367.

Pavlides, S.B. and Valkaniotis, S., 2003. Tectonic regime of Santorini-Amorgos area, *Proceedings of International Conference "The South Aegean Active Volcanic Arc: Present Knowledge and Future Perspectives", Milos Island, Greece 17-20 September 2003,* p.76.

Pavlis, G. L., 1986. Appraising earthquake hypocenter location errors: a complete, practical approach for single-event locations. *Bull. Seism. Soc. Am. 76*, pp. 1699-1717.

Perissoratis, C., 1990. Marine geological research on Santorini: preliminary results. *In: D.A. Hardy (Editor), Thera and the Aegean World, III. The Thera Foundation, London*, pp. 300-304.

Perissoratis, C. 1995. The Santorini volcanic complex and its relation to the stratigraphy and structure of the Aegean arc, Greece. *Marine Geology, 128*, pp. 37-58.

Perissoratis, C. and Papadopoulos, G. 1999. Sediment instability and slumping in the southern Aegean Sea and the case history of the 1956 tsunami. *Marine Geology, 161*, pp. 287-305.

Piper, D.J.W. and Perissoratis, C., 2003. Quaternary neotectonics of the South Aegean arc. *Marine Geology, 198*, pp. 259-288.

Piper D.J.W., Pe-Piper G., Perissoratis C. and Anastasakis G. 2004. Submarine volcanic rocks around Santorini and their relationship to faulting. *Proceedings of the 5th International Symposium on Eastern Mediterranean Geology, Thessaloniki, Greece, 14-20 April 2004,* pp. 873-876.

Poupinet, G., Ellsworth, W. L. and Fréchet, J., 1984. Monitoring velocity variations in the crust using earthquake doublets: An application to the Calaveras Fault, California. *J. Geophys. Res., 89,* pp. 5719– 5731.

Reasenberg, P.A. and D. Oppenheimer 1985. FPFIT, FPPLOT and FPPAGE: FORTRAN computer programs for calculating and displaying earthquake fault-plane solutions. *U.S. Geological Survey Open-File Report 85-739*.

Roecker, S.W., 1982. Velocity Structure of the Pamir-Hindu Kush Region: Possible evidence of subducted crust. *Journal of Geophysical Research 87,* pp. 945-95

Sigurdsson, H., Carey, S., Alexandri, M., Vougioukalakis, G., Croff, K., Roman, C., Sakellariou, D., Anagnostou, C., Rousakis, G., Ioakim, C., Gogou, A., Ballas, D., Misaridis, T., and P., Nomikou, 2006. Marine Investigations of Greece's Santorini Volcanic Field. *EOS, Vol. 87, No. 34, 22 August 2006*, pp. 337-348.

Shirokova, E.I., 1972. Stress pattern and probable motion in the earthquake foci of the Asia-Mediterranean seismic belt. *In: L.M. Balakina et al. (Editors), Elastic Strain Field of the Earth and Mechanisms of Earthquake Sources. Nauka, Moscow,* p. 8.

Tapley, W.C. and J.E. Tull, 1992. SAC – Seismic Analysis Code: Users Manual. *Lawrence Livermore National Laboratory*, *Revision 4,* pp 388.

Thurber, C.H., 1983. Earthquake Locations and Three-Dimensional Crustal Structure in the Coyote Lake Area, Central California. *Journal of Geophysical Research 88*, pp. 8226-8236.

Tull, J.E., 1987. SAC – Seismic Analysis Code: Tutorial guide for new users. *Lawrence Livermore National Laboratory, Livermore, CA.* UCRL-MA-112835.

Vougioukalakis, G., Francalanci, L., Sbrana, A. and Mitropoulos, D., 1995. The 1649-1650 Kolumbo submarine volcano activity, Santorini, Greece. *In: F. Barberi, R. Casale and M. Frata (Editors), "The European Laboratory Volcanoes, Workshop Proceeding", European Commission, European Science Foundation, Luxemburg*, pp. 189-192.

Waldhauser, F., 2001. HypoDD: A computer program to compute double-difference hypocenter locations, *U.S. Geol. Surv. Open File Rep., 01-113*, pp. 25.

Waldhauser, F. and Ellsworth, W. L., 2000. A double-difference earthquake location algorithm: Method and application to the northern Hayward Fault, California. *Bull. Seismol. Soc. Am., 90*, pp 1353– 1368.

Waldhauser, F. and Ellsworth, W. L., 2002. Fault structure and mechanics of the Hayward Fault, California, from double-difference earthquake locations. *Journal of Geophysical Research, Vol. 107, No. 3, 2054*, pp. 1-15.

Waldhauser, F., Ellsworth, W. L. and Cole, A., 1999. Slip-parallel seismic lineations along the northern Hayward Fault, California. *Geophys. Res. Lett., 26,* pp. 3525–3528.

Zellmer, G., Annen, C., Charlier, B. L. A., George, R. M. M., S. P. Turner and C. J. Hawkesworth, 2005. Magma evolution and ascent at volcanic arcs: constraining petrogenetic processes through rates and chronologies. *Journal of Volcanology and Geothermal Research 140*, pp. 171-191.